

Enhancement of Kondo effect in multilevel quantum dots

Mikio ETO*

Faculty of Science and Technology, Keio University, 3-14-1 Hiyoshi, Kohoku-ku, Yokohama 223-8522, Japan

(Received July 17, 2004)

We theoretically study enhancement mechanisms of the Kondo effect in multilevel quantum dots. In quantum dots fabricated on semiconductors, the energy difference between discrete levels Δ is tunable by applying a magnetic field. With two orbitals and spin 1/2 in the quantum dots, we evaluate the Kondo temperature T_K as a function of Δ , using the scaling method. T_K is maximal around $\Delta = 0$ and decreases with increasing $|\Delta|$, following a power law, $T_K(\Delta) = T_K(0) \cdot (T_K(0)/|\Delta|)^\gamma$, which is understood as a crossover from SU(4) to SU(2) Kondo effect. The exponents on both sides of a level crossing, γ_L and γ_R , satisfy a relation of $\gamma_L \cdot \gamma_R = 1$. We compare this enhanced Kondo effect with that by spin-singlet-triplet degeneracy for an even number of electrons, to explain recent experimental results using vertical quantum dots.

KEYWORDS: quantum dot, Kondo effect, multilevel, scaling method

1. Introduction

Kondo effect is one of the most important many-body problems in solid-state physics.¹⁾ When a localized spin ($S = 1/2$) is brought in contact with electron Fermi sea, the Kondo effect gives rise to a new many-body ground state of a spin singlet and markedly influences the transport properties.^{2,3)} The Kondo effect was originally discovered in metals including dilute magnetic impurities. The Kondo effect also takes place in semiconductor quantum dots connected to external leads through tunnel barriers, as predicted by several theoretical groups.⁴⁻⁹⁾ In this case, a localized spin S is formed by electrons confined in the quantum dots due to the Coulomb blockade.¹⁰⁾ Usually, the spin is zero or 1/2 in the Coulomb blockade region with an even and odd number of electrons, respectively, since discrete spin-degenerate levels are consecutively occupied in the quantum dots. Hence the Kondo effect is observed in the latter case only.¹¹⁻¹³⁾

The semiconductor quantum dots offer the following merits for the investigation of the Kondo physics. First, we can examine the properties of single “magnetic impurity.” Second, the transport of conduction electrons is observed through the magnetic impurity in the case of quantum dots, whereas the scattering by the magnetic impurities is observed in the traditional metallic systems. In the former, the resonant nature of the Kondo effect is directly detected: The conductance is enhanced to a universal value of $2e^2/h$ at temperatures much below the Kondo temperature, T_K ,¹⁴⁾ which is ascribable to the resonant tunneling through Kondo singlet state. In the latter, the electric resistance is anomalously enhanced at low temperatures since the scattering probability is amplified by the resonance. This explains a “resistance minimum” as a function of temperature (T), together with the resistivity due to the phonons which increases with T .¹⁾ (In the Coulomb blockade region of quantum dots, the normal conductance increases with T by the thermal activation. Thus the Kondo effect results in a “conductance minimum.”) Third, various parameters are tunable in quantum dots using gate electrodes, *e.g.*, number of electrons, strength of tunnel coupling. Nonequilibrium

* E-mail address: eto@rk.phys.keio.ac.jp

situations are also realized by applying a finite bias voltage.

Besides the conventional Kondo effect with spin 1/2, unconventional Kondo effects have been discovered which stem from the interplay between spin and orbital degrees of freedom in quantum dots. An example is the enhanced Kondo effect at the energy degeneracy between spin-singlet and -triplet states for an even number of electrons (S-T Kondo effect).¹⁵⁾ In vertically fabricated quantum dots, the spacing between discrete levels can be tuned by applying a magnetic field perpendicularly to the quantum dots. Around a level degeneracy, high-spin states appear by the exchange interaction (Hund's rule).¹⁶⁾ Hence the energy difference Δ between spin-singlet and -triplet states is tunable by the magnetic field, as schematically shown in Fig. 1(b). The Kondo effect is significantly enhanced around $\Delta = 0$. Note that the Zeeman effect is irrelevant in the experiment since the Zeeman energy is much smaller than T_K , owing to a small g factor in semiconductors. This S-T Kondo effect has been explained theoretically by the author and Nazarov¹⁷⁻¹⁹⁾ and by Pustilnik and Glazman.^{20,21)} (The Zeeman effect is relevant to the S-T Kondo effect in carbon nanotubes.²²⁾ We refer to ref. 23 for the theoretical study.)

Recently another large Kondo effect has been found around the two-orbital degeneracy for an odd number of electrons with spin 1/2 [doublet-doublet (D-D) Kondo effect].²⁴⁾ When the energy difference between the two orbitals Δ is tuned [Fig. 1(a)], the conductance is largely enhanced around $\Delta = 0$ by the Kondo effect. Though the Kondo effect is expected with single level and spin 1/2, the Kondo temperature is probably smaller than actual temperature T so that no conductance increase is seen except the vicinity of the level crossing point in this experiment. Around $\Delta = 0$, the estimated T_K is similar to that for the S-T Kondo effect observed in the same samples, indicating that a total of fourfold spin and orbital degeneracy contributes to enhance T_K in both the cases.

The purpose of the present paper is to study the D-D Kondo effect theoretically and to elucidate the differences between D-D and S-T Kondo effects. It is known that the orbital degeneracy plays an important role in the Kondo effect of magnetic impurities with f electrons. When the total degeneracy factor is $N_d = 2j + 1$ (j is the total angular momentum consisting of orbital angular momentum and spin), the Kondo effect is described by the Coqblin-Schrieffer model of $SU(N_d)$ symmetry.^{2,25)} This model yields the Kondo temperature of $T_K \sim D_0 e^{-1/N_d \nu J}$ with exchange coupling J , where D_0 and ν are the bandwidth and density of states of conduction electrons, respectively. Hence the degeneracy factor N_d significantly enhances the Kondo temperature. We examine the Kondo effect in quantum dots with two orbitals and spin 1/2 and evaluate the Kondo temperature as a function of Δ . We find that T_K is maximal around $\Delta = 0$ and decreases with increasing $|\Delta|$ by a power law, $T_K(\Delta) = T_K(0) \cdot (T_K(0)/|\Delta|)^\gamma$, with exponent $\gamma = 1$. This behavior of T_K is understood as a crossover from $SU(4)$ to $SU(2)$ Kondo effect when the strength of the tunnel coupling is equivalent for the two orbitals. Since the spin-orbit interaction can be disregarded in the quantum dots, the degenerate factor is $N_d = 4$ ($N_d = 2$) for orbital and spin degrees of freedom when $\Delta = 0$ ($\Delta \neq 0$). In general situations, the exponent of the power law is not a universal value since the fixed point of $SU(4)$ Kondo effect is marginal. We find a relation of $\gamma_L \cdot \gamma_R = 1$, where γ_L and γ_R are the exponents on both sides of a level crossing. The Δ dependence of T_K was not studied in details by previous theoretical works on the Kondo effect in multilevel quantum dots.²⁶⁻³⁰⁾

The behavior of $T_K(\Delta)$ in the D-D Kondo effect is similar to that in the S-T Kondo effect.¹⁷⁻²¹⁾ We clarify the differences between them to explain the above-mentioned experimental results.²⁴⁾

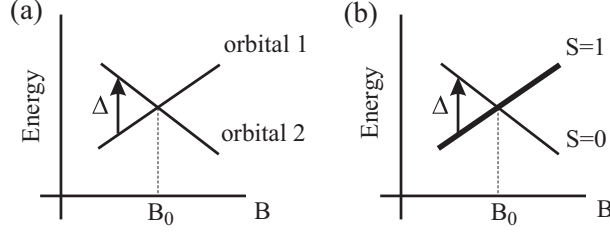


Fig. 1. In a quantum dot with two orbitals, the energy difference Δ can be tuned using a magnetic field B . (a) $\Delta = \varepsilon_2 - \varepsilon_1$, level spacing between the two orbitals for an electron in the quantum dot, and (b) $\Delta = E_{S=0} - E_{S=1}$, the energy difference between spin-singlet and -triplet states for two electrons.

Our discussion is restricted to the case of quantum dots vertically fabricated from double-barrier heterostructures.^{10,15,16,24)} In transport processes between a quantum dot and leads through heterostructure tunnel junctions, the orbital quantum numbers are conserved for the motion of electrons in the transverse direction. Therefore there are two channels of conduction electrons in the leads when two orbitals are relevant in the quantum dot; each channel couples to only one of the two orbitals. The situation is different in quantum dots of lateral geometry, in which a single channel in each lead couples to both the orbitals through a tunnel junction.¹⁰⁾ We refer to refs. 31 and 32–34 for experimental and theoretical studies on the S-T Kondo effect in lateral quantum dots.

The organization of the present paper is as follows. In the next section (§2), we model a quantum dot with two orbitals and spin 1/2 for the D-D Kondo effect. In §3, the Kondo temperature is evaluated as a function of energy difference Δ between the two orbitals, using the scaling method. In §4, the scaling analysis is given for the S-T Kondo effect, according to our previous works.^{17–19)} The final section (§5) is devoted to conclusions and discussion. We compare the D-D and S-T Kondo effects to explain the experimental results.²⁴⁾

2. Model

As a model for the D-D Kondo effect, we consider a quantum dot with an electron ($S = 1/2$) and two orbitals ($i = 1, 2$). The energy difference between the orbitals is denoted by $\Delta = \varepsilon_2 - \varepsilon_1$. The Hamiltonian in the quantum dot reads

$$H_{\text{dot}} = \sum_{\mu} \varepsilon_i d_{\mu}^{\dagger} d_{\mu} + E_c (\hat{n} - \mathcal{N}_{\text{gate}})^2, \quad (1)$$

where d_{μ}^{\dagger} and d_{μ} are creation and annihilation operators of the dot state $\mu = (i, S_z)$, respectively. $\hat{n} = \sum_{\mu} d_{\mu}^{\dagger} d_{\mu}$ is the number operator of electrons in the quantum dot. E_c is the charging energy, whereas $\mathcal{N}_{\text{gate}}$ is tuned by the gate voltage. We set $\mathcal{N}_{\text{gate}} = 1$ for the Coulomb blockade region with an electron in the quantum dot. The exchange interaction between electrons in the quantum dot is neglected in sections 2 and 3 since it is irrelevant to the D-D Kondo effect.

The quantum dot is connected to two external leads, L and R , through tunnel barriers. We assume that the orbital symmetry is conserved in the tunnel processes, which is the case of vertical quantum dots. Hence the leads have two channels; channel i ($= 1, 2$) in lead L (R) couples to orbital i by $V_{L,i}$ ($V_{R,i}$). We perform a unitary transformation for conduction electrons in the two leads, along the lines of ref. 4;

$$c_{k\mu} = (V_{L,i}^* c_{L,k\mu} + V_{R,i}^* c_{R,k\mu}) / V_i,$$

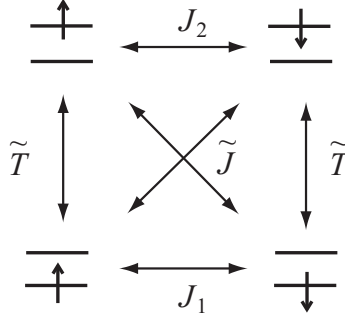


Fig. 2. Four states in a quantum dot with an electron ($S = 1/2$) and two orbitals ($i = 1, 2$). There are exchange processes among them (J_1 , J_2 , \tilde{T} and T) due to the second-order tunnel couplings with conduction electrons in the leads.

$$\bar{c}_{k\mu} = (-V_{R,i}c_{L,k\mu} + V_{L,i}c_{R,k\mu})/V_i,$$

with $V_i = \sqrt{|V_{L,i}|^2 + |V_{R,i}|^2}$, where $c_{\alpha,k\mu}$ is the annihilation operator of an electron in lead α , with momentum k and $\mu = (i, S_z)$. The mode $c_{k\mu}$ is coupled to the quantum dot with V_i , whereas the mode $\bar{c}_{k\mu}$ is decoupled and thus shall be disregarded. The Hamiltonian of the leads and that of tunnel processes are written as

$$H_{\text{leads}} = \sum_k \sum_{\mu} \varepsilon_k c_{k\mu}^{\dagger} c_{k\mu}, \quad (2)$$

$$H_T = \sum_k \sum_{\mu} V_i (c_{k\mu}^{\dagger} d_{\mu} + \text{h.c.}), \quad (3)$$

respectively.

We define addition and extraction energies as the energy cost to add or subtract an electron on/from the quantum dot, $E^+ = \varepsilon_1 + E_c - E_F$, $E^- = E_F - \varepsilon_1$, where E_F is the Fermi level in the leads. We assume that $E^{\pm} \gg |\Delta|$. The level broadening of orbital i is given by $\Gamma_i = \pi\nu V_i^2$, where ν is the density of states in the leads. The level broadening and temperature T should be much smaller than E^{\pm} for the Coulomb blockade.

Considering the second-order tunnel processes, H_T , we obtain the effective Hamiltonian H_{eff} in a subspace with one electron in the quantum dot. We introduce the pseudofermion operators f_{μ}^{\dagger} (f_{μ}) that create (annihilate) the dot state $\mu = (i, S_z)$. The constraint of

$$\sum_{\mu} f_{\mu}^{\dagger} f_{\mu} = 1 \quad (4)$$

is required. The Hamiltonian is written as

$$\begin{aligned} H_{\text{eff}} &= \sum_{\mu} \varepsilon_i f_{\mu}^{\dagger} f_{\mu} + H_{\text{lead}} \\ &+ 2J_1 \mathbf{s}^{(1)} \cdot \mathbf{S}^{(1)} + 2J_2 \mathbf{s}^{(2)} \cdot \mathbf{S}^{(2)} \\ &+ 2\tilde{J} [\mathbf{s}^{(12)} \cdot \mathbf{S}^{(21)} + \mathbf{s}^{(21)} \cdot \mathbf{S}^{(12)}] \\ &+ 2\tilde{T} \left[\left(\sum_{kk'} \sum_s c_{k',1,s}^{\dagger} c_{k,2,s} \right) \left(\sum_s f_{2,s}^{\dagger} f_{1,s} \right) + \text{h.c.} \right] \\ &+ 2T \left[\sum_{kk'} \sum_s (c_{k',1,s}^{\dagger} c_{k,1,s} - c_{k',2,s}^{\dagger} c_{k,2,s}) \right] \left[\sum_s (f_{1,s}^{\dagger} f_{1,s} - f_{2,s}^{\dagger} f_{2,s}) \right], \end{aligned} \quad (5)$$

where

$$\begin{aligned}
\mathbf{s}^{(i)} &= \sum_{kk'} \sum_{ss'} c_{k',i,s'}^\dagger (\boldsymbol{\sigma}_{s's}/2) c_{k,i,s}, \\
\mathbf{S}^{(i)} &= \sum_{ss'} f_{i,s'}^\dagger (\boldsymbol{\sigma}_{s's}/2) f_{i,s}, \\
\mathbf{s}^{(ij)} &= \sum_{kk'} \sum_{ss'} c_{k',i,s'}^\dagger (\boldsymbol{\sigma}_{s's}/2) c_{k,j,s}, \\
\mathbf{S}^{(ij)} &= \sum_{ss'} f_{i,s'}^\dagger (\boldsymbol{\sigma}_{s's}/2) f_{j,s}.
\end{aligned}$$

The third (fourth) term in H_{eff} represents the exchange coupling between conduction electrons of channel 1 (2) and dot spin 1/2 at orbital 1 (2). The terms with \tilde{J} and \tilde{T} describe the interchannel scattering of conduction electrons by the dot electron with or without spin flip. The coupling constants are given by $J_1 = V_1^2/\tilde{E}_C$, $J_2 = V_2^2/\tilde{E}_C$ and $\tilde{J} = \tilde{T} = V_1 V_2/\tilde{E}_C$, where $1/\tilde{E}_C = 1/E^+ + 1/E^-$. These processes are schematically shown in Fig. 2. A potential scattering term with $T = (V_1^2 + V_2^2)/(2\tilde{E}_C)$ is also relevant to the Kondo effect, whereas irrelevant potential scatterings are disregarded in H_{eff} .

In the case of $V_1 = V_2$, all the coupling constants are identical to one another, $J_1 = J_2 = \tilde{J} = \tilde{T} = T \equiv J$. Then the effective Hamiltonian is reduced to the Coqblin-Schrieffer model of SU(4) symmetry if $\Delta = 0$. Indeed, using a pseudospin $T_z = \pm 1/2$ to represent orbitals $i = 1, 2$, H_{eff} is rewritten as

$$H_{\text{eff}} = H_{\text{lead}} + J \mathbf{S} \cdot \mathbf{s} - \tilde{\mathbf{B}} \cdot \mathbf{S}, \quad (6)$$

where

$$\begin{aligned}
\mathbf{S} &= \frac{1}{2} \sum_{\mu\nu} f_\mu^\dagger \hat{\Sigma}_{\mu\nu} f_\nu, \\
\mathbf{s} &= \frac{1}{2} \sum_{kk'} \sum_{\mu\nu} c_{k',\mu}^\dagger \hat{\Sigma}_{\mu\nu} c_{k,\nu}.
\end{aligned}$$

$\hat{\Sigma}$ involves 15 components which are generators of the Lie algebra $\text{su}(4)$, $\{(\tau_x, \tau_y, \tau_z, I) \otimes (\sigma_x, \sigma_y, \sigma_z, I)\} - \{I \otimes I\}$, where σ_i (τ_i) are the Pauli matrices in the spin (pseudospin) space and I is the unit matrix. The energy difference Δ is expressed by the fictitious magnetic field $\tilde{\mathbf{B}}$, the $\tau_z \otimes I$ component of which is Δ and the other components are 0:

$$\tilde{\mathbf{B}} \cdot \mathbf{S} = \frac{\Delta}{2} \sum_s (f_{1,s}^\dagger f_{1,s} - f_{2,s}^\dagger f_{2,s}).$$

When $\tilde{\mathbf{B}} = 0$, the Hamiltonian (6) is invariant with respect to the rotation in a product space of spin and pseudospin spaces [SU(4) symmetry].

3. Scaling calculations

To evaluate the Kondo temperature, the effective Hamiltonian, (5) or (6), is analyzed using “poor man’s” scaling method.^{35–37} We assume that the density of states of conduction electrons in the leads is constant ν in the energy range $[-D, D]$. With changing the bandwidth from D to

$D - |dD|$, we renormalize the exchange coupling constants ($J_1, J_2, \tilde{J}, \tilde{T}, T$) not to change the low-energy physics, within the second-order perturbation with respect to the exchange couplings. This procedure yields the scaling equations in two limits, $D \gg |\Delta|$ and $D \ll |\Delta|$. The Kondo temperature T_K is determined as the energy scale D at which the coupling constants become so large that the perturbation breaks down.

3.1 $SU(4)$ Kondo effect

We begin with the case of $V_1 = V_2$, where $J_1 = J_2 = \tilde{J} = \tilde{T} = T \equiv J$. Using the Hamiltonian (6), we obtain the scaling equations for a single coupling constant J .

When the energy scale D is much larger than the energy difference $|\Delta|$, the scaling equation is given by

$$dJ/d\ln D = -4\nu J^2. \quad (7)$$

The exchange coupling J develops rapidly with decreasing D , reflecting a fourfold degeneracy of spin and pseudospin. This represents the $SU(4)$ Kondo effect.

When $D \ll |\Delta|$, the equation is

$$dJ/d\ln D = -2\nu J^2. \quad (8)$$

The evolution of J is slower since one component of T_z (orbital of the upper level) is irrelevant. This is the conventional Kondo effect of $SU(2)$ symmetry.

From these equations, we evaluate the Kondo temperature T_K as a function of Δ . (i) T_K is maximal around $\Delta = 0$ [$|\Delta| \ll T_K(\Delta = 0)$]. In this case, the scaling equation (7) remains valid till the scaling ends. This yields

$$T_K(\Delta = 0) = D_0 \exp[-1/4\nu J], \quad (9)$$

where D_0 is the initial bandwidth and given by $D_0 = \sqrt{E_+ E_-}$.³⁸⁾

(ii) T_K is minimal when $|\Delta| \gg D_0$. Then eq. (8) is valid in the whole scaling region. Solving the equation, we obtain

$$T_K(\Delta = \infty) = D_0 \exp[-1/2\nu J]. \quad (10)$$

(iii) The intermediate region of $T_K(0) \ll |\Delta| \ll D_0$ is examined as follows. With decreasing the energy scale D , the renormalization flow goes toward the fixed point of $SU(4)$ Kondo effect first [eq. (7) for $D \gg |\Delta|$], and then goes to the fixed point of $SU(2)$ Kondo effect [eq. (8) for $D \ll |\Delta|$]. To consider this crossover behavior, we match the solutions of eqs. (7) and (8) at $D \approx |\Delta|$. We find that $T_K(\Delta)$ decreases with increasing $|\Delta|$, following a power law,

$$T_K(\Delta) = T_K(0) \cdot (T_K(0)/|\Delta|)^\gamma, \quad (11)$$

with exponent $\gamma = 1$. Our results of (i), (ii) and (iii) clearly indicate an enhancement of the Kondo effect around $\Delta = 0$ [see Fig. 6(a) for the schematic drawing of $T_K(\Delta)$], in accordance with the experimental observation.²⁴⁾

The expression of $T_K(\Delta)$, eq. (11), has been originally derived by Yamada *et al.* for the Kondo effect in metals with magnetic impurities in the presence of a crystal field.³⁹⁾ The exact solution of this Kondo effect has also been obtained.^{40,41)} Lately Borda *et al.* has examined the $SU(4)$ Kondo effect in a double quantum dot system with interdot capacitive coupling.⁴²⁾ Their model is equivalent to ours when the tunnel coupling is absent between the double dots. [The magnetic field

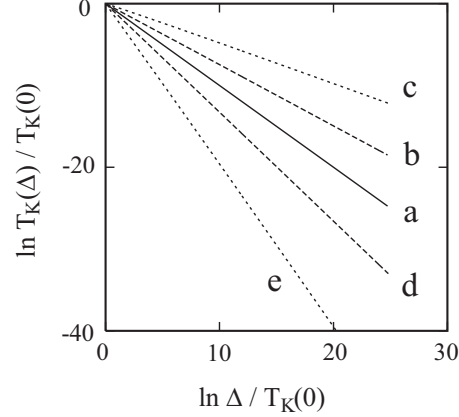


Fig. 3. Calculated results of the Kondo temperature T_K for the D-D Kondo effect, as a function of energy difference Δ between the two orbitals, on a log-log scale. Both T_K and Δ are normalized by the Kondo temperature at $\Delta = 0$, $T_K(0)$. (a) $(V_2/V_1)^2 = 1$, (b) $3/4$, (c) $1/2$, (d) $4/3$ and (e) 2 . The scaling equations, (12) for $D > \Delta$ and (13) for $D < \Delta$, are solved numerically with the initial condition of $\nu(J_1 + J_2) = 0.02$.

in ref. 42 corresponds to $\tilde{\mathbf{B}}$ in eq. (6).] Using numerical renormalization group calculations, they have estimated T_K as a function of magnetic field and shown its enhancement around the fourfold degeneracy. This is in qualitative agreement with our scaling results.

3.2 General case of $V_1 \neq V_2$

Now we examine general situations of $V_1 \neq V_2$. We set $\Delta = \varepsilon_2 - \varepsilon_1 \geq 0$ in this subsection. We derive a set of scaling equations for J_1 , J_2 , \tilde{J} , \tilde{T} and T in Hamiltonian (5), using the poor man's scaling method. For $D \gg \Delta$,

$$\begin{cases} dJ_1/\nu d \ln D &= -2J_1^2 - \tilde{J}(\tilde{J} + \tilde{T}), \\ dJ_2/\nu d \ln D &= -2J_2^2 - \tilde{J}(\tilde{J} + \tilde{T}), \\ d\tilde{J}/\nu d \ln D &= -\tilde{J}(J_1 + J_2 + T) - \tilde{T}(J_1 + J_2)/2, \\ d\tilde{T}/\nu d \ln D &= -3\tilde{J}(J_1 + J_2)/2 - \tilde{T}T, \\ dT/\nu d \ln D &= -3\tilde{J}^2 - \tilde{T}^2. \end{cases} \quad (12)$$

For $D \ll \Delta$,

$$dJ_1/d \ln D = -2\nu J_1^2, \quad (13)$$

whereas the other coupling constants do not evolve.

Analyzing eqs. (12), we find that the fixed point of SU(4) Kondo effect, $J_1 = J_2 = \tilde{J} = \tilde{T} = T = \infty$, is marginal (Appendix A). With a decrease in D , a marginal variable, $(J_1 - J_2)/(J_1 + J_2)$, is almost kept at the initial value while the other variables are renormalized toward the values at the fixed point. In consequence, $T_K(\Delta)$ is not a universal function although T_K is always maximal around $\Delta = 0$.

To examine $T_K(\Delta)$, we numerically solve the scaling equations, eqs. (12) for $D > \Delta$ and eq. (13) for $D < \Delta$. We put $\nu(J_1 + J_2) = 0.02$ in the initial condition and determine the Kondo temperature T_K as the energy scale D at which νJ_1 becomes as large as unity. The calculated results of $T_K(\Delta)$ are shown in Fig. 3 on a log-log scale, with (a) $(V_2/V_1)^2 = 1$, (b) $3/4$, (c) $1/2$, (d) $4/3$ and (e) 2 . $T_K(\Delta)$ seems to follow a power law

$$T_K(\Delta) = T_K(0) \cdot (T_K(0)/\Delta)^\gamma, \quad (14)$$

but the exponent depends on model parameters. It is approximately given by

$$\gamma = \left(\frac{V_2}{V_1} \right)^2 = \frac{\Gamma_2}{\Gamma_1}, \quad (15)$$

as long as $\Gamma_1 \sim \Gamma_2$ (Appendix A). If $\Gamma_2/\Gamma_1 \gg 1$ or $\ll 1$, $T_K(\Delta)$ deviates from the power law. Then the renormalization of Δ ,⁴³⁾ that is not considered in our calculations, might have to be taken into account to determine T_K , besides the renormalization of exchange couplings.

If we denote the exponents on the left and right sides of a level crossing in Fig. 1(a) by γ_L and γ_R , respectively, we obtain a general relation of

$$\gamma_L \cdot \gamma_R = \frac{\Gamma_2}{\Gamma_1} \cdot \frac{\Gamma_1}{\Gamma_2} = 1,$$

since the roles of orbitals 1 and 2 are interchanged at the level crossing.

4. Singlet-triplet Kondo effect

We examine the Kondo effect around the singlet-triplet degeneracy for an even number of electrons in this section. In our previous papers,^{17–19)} the scaling analysis has been presented for this S-T Kondo effect in vertical quantum dots in rectangular shape.¹⁵⁾ Here, the analysis is modified for circular quantum dots used in the experiment of ref. 24.

We consider a quantum dot with two orbitals and two electrons. The exchange interaction which favors parallel spins,

$$-E_{\text{ex}} \sum_{s_1 s_2 s_3 s_4} (\boldsymbol{\sigma}/2)_{s_1 s_2} \cdot (\boldsymbol{\sigma}/2)_{s_3 s_4} d_{1,s_1}^\dagger d_{1,s_2} d_{2,s_3}^\dagger d_{2,s_4}$$

with $\boldsymbol{\sigma} = (\sigma_x, \sigma_y, \sigma_z)$, is important in this problem. We add this term to the dot Hamiltonian (1) and fix $\mathcal{N}_{\text{gate}} = 2$ for the Coulomb blockade with two electrons in the quantum dot. The possible ground state is a spin singlet ($S = 0$) or triplet ($S = 1$, $S_z \equiv M = 1, 0, -1$). We denote the states by $|SM\rangle$,

$$\begin{aligned} |00\rangle &= d_{1\uparrow}^\dagger d_{1\downarrow}^\dagger |0\rangle, \\ |11\rangle &= d_{1\uparrow}^\dagger d_{2\uparrow}^\dagger |0\rangle, \\ |10\rangle &= \frac{1}{\sqrt{2}} (d_{1\uparrow}^\dagger d_{2\downarrow}^\dagger + d_{1\downarrow}^\dagger d_{2\uparrow}^\dagger) |0\rangle, \\ |1-1\rangle &= d_{1\downarrow}^\dagger d_{2\downarrow}^\dagger |0\rangle, \end{aligned}$$

where $|0\rangle$ represents the vacuum, assuming $\varepsilon_1 < \varepsilon_2$.⁴⁴⁾ The energy difference between them is $E_{S=0} - E_{S=1} = E_{\text{ex}} - (\varepsilon_2 - \varepsilon_1)$, which is denoted by Δ in this section. We disregard two other singlet states, $d_{2\uparrow}^\dagger d_{2\downarrow}^\dagger |0\rangle$ and $(1/\sqrt{2})(d_{1\uparrow}^\dagger d_{2\downarrow}^\dagger - d_{1\downarrow}^\dagger d_{2\uparrow}^\dagger) |0\rangle$, since they have larger energies than state $|00\rangle$. We assume that addition and extraction energies, E^\pm , are much larger than $|\Delta|$ and level broadenings, Γ_1, Γ_2 .

As in §2, we make an effective Hamiltonian H_{eff} in a space of two-electron states, $|00\rangle$, $|11\rangle$, $|10\rangle$ and $|1-1\rangle$, taking account of the second-order tunnel processes, H_T . The Hamiltonian reads

$$H_{\text{eff}} = H_{\text{dot}} + H_{\text{leads}} + H^{S=1} + H^{S=1 \leftrightarrow 0} + H_{\text{pot}}. \quad (16)$$

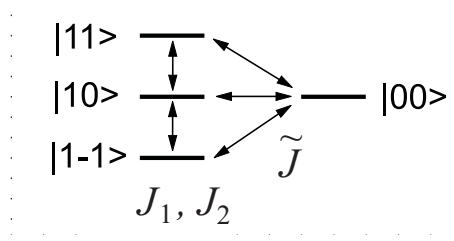


Fig. 4. Four states that we consider in a quantum dot with two orbitals and two electrons, $|S, M\rangle$, and exchange processes among them. The exchange process denoted by J_1 (J_2) is accompanied by a spin-flip scattering of conduction electrons of channel 1 (2), whereas that by \tilde{J} is accompanied by an interchannel scattering of conduction electrons.

The first term represents the dot state,

$$H_{\text{dot}} = \sum_{S,M} E_S f_{SM}^\dagger f_{SM}, \quad (17)$$

using pseudofermion operators f_{SM}^\dagger (f_{SM}) which create (annihilate) the state $|SM\rangle$. It is required that

$$\sum_{SM} f_{SM}^\dagger f_{SM} = 1. \quad (18)$$

$H^{S=1}$ describes the spin-flip processes among three components of the triplet state, $|11\rangle$, $|10\rangle$ and $|1-1\rangle$, with a scattering of conduction electrons of channel 1 or 2. The coupling constants are given by $J_1 = V_1^2/(2\tilde{E}_C)$ and $J_2 = V_2^2/(2\tilde{E}_C)$, respectively, where $1/\tilde{E}_C = 1/E^+ + 1/E^-$. $H^{S=1 \leftrightarrow 0}$ represents the conversion between the triplet and singlet states with an interchannel scattering of conduction electrons. The coupling constant is $\tilde{J} = V_1 V_2/(\sqrt{2}\tilde{E}_C)$. These spin-flip processes are schematically shown in Fig. 4. A potential scattering H_{pot} with $T = (V_1^2 + V_2^2)/(2\tilde{E}_C)$ is also relevant to the S-T Kondo effect. (See ref. 19 for explicit expressions of the Hamiltonian.)

We obtain the scaling equations for the coupling constants, J_1 , J_2 , \tilde{J} , T , using the poor man's scaling method. When $D \gg |\Delta|$,

$$\begin{cases} dJ_1/\nu d \ln D &= -2J_1^2 - \tilde{J}^2, \\ dJ_2/\nu d \ln D &= -2J_2^2 - \tilde{J}^2, \\ d\tilde{J}/\nu d \ln D &= -2(J_1 + J_2)\tilde{J} - T\tilde{J}, \\ dT/\nu d \ln D &= -8\tilde{J}^2. \end{cases} \quad (19)$$

These equations have a stable fixed point of $J_1 = J_2 = \infty$, $\tilde{J}/J_1 = \sqrt{2(2 + \sqrt{5})}$ and $T/J_1 = 2(1 + \sqrt{5})$ (Appendix B). The renormalization flow of the exchange couplings goes toward this fixed point, as the energy scale D decreases.

When $D \ll \Delta$, the singlet state can be safely disregarded. The scaling equations are given by

$$\begin{cases} dJ_1/d \ln D &= -2\nu J_1^2, \\ dJ_2/d \ln D &= -2\nu J_2^2, \end{cases} \quad (20)$$

indicating that J_1 and J_2 evolve independently. The other coupling constants do not change. On the singlet side ($\Delta < 0$), all the exchange couplings saturate, provided $D \ll |\Delta|$.

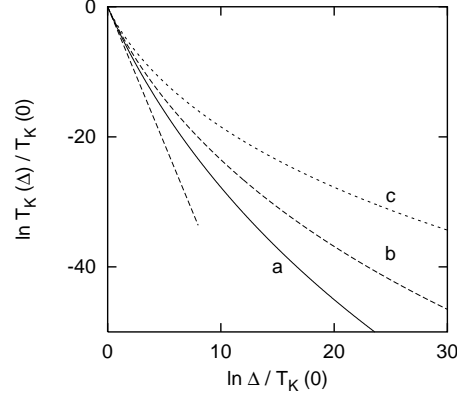


Fig. 5. Calculated results of the Kondo temperature T_K for the S-T Kondo effect, as a function of the energy difference Δ between spin-singlet and -triplet states, on a log-log scale. Both T_K and Δ are normalized by the Kondo temperature at $\Delta = 0$, $T_K(0)$. (a) $(V_2/V_1)^2 = 1$, (b) $3/4$ or $4/3$, and (c) $1/2$ or 2 . The scaling equations, (19) for $D > \Delta$ and (20) for $D < \Delta$, are solved numerically with the initial condition of $\nu(J_1 + J_2) = 0.01$. A straight broken line indicates a slope of $\gamma = 2 + \sqrt{5} \approx 4.2$.

The Kondo temperature T_K is evaluated as a function of Δ , in the same way as in §3. (i) When $|\Delta| \ll T_K(0)$, the scaling equations (19) are valid till the end of the scaling. Then T_K is maximal although the analytical expression of $T_K(0)$ cannot be obtained.⁴⁵⁾

(ii) When $\Delta > D_0$, the ground state is a spin triplet, whereas the singlet state is not relevant to the Kondo effect. Then the scaling equations (20) work in the whole scaling region. This yields

$$T_K(\infty) = D_0 \exp[-1/2\nu J_1], \quad (21)$$

when $J_1 \geq J_2$ (J_1 should be replaced by J_2 when $J_1 < J_2$). This is the Kondo temperature of a localized spin with $S = 1$.⁴⁶⁾

(iii) In the intermediate region of $T_K(0) \ll \Delta \ll D_0$, all the coupling constants develop with decreasing D , following eq. (19) when $D \gg \Delta$. \tilde{J} and T saturate at $D \approx \Delta$, whereas J_1 and J_2 continue to grow by eq. (20) when $D \ll \Delta$. To see the Δ dependence of T_K , we perform numerical calculations.¹⁹⁾ We solve eqs. (19) and (20) for $D > \Delta$ and $D < \Delta$, respectively, with the initial condition of $\nu(J_1 + J_2) = 0.01$. The Kondo temperature T_K is determined as the energy scale D at which $\nu J_1 = 1$ or $\nu J_2 = 1$. The calculated results of $T_K(\Delta)$ are shown in Fig. 5 on a log-log scale, with (a) $J_2/J_1 = (V_2/V_1)^2 = 1$, (b) $3/4$ or $4/3$, and (c) $1/2$ or 2 . $T_K(\Delta)$ shows the power law of eq. (14) with an exponent of $\gamma = 2 + \sqrt{5}$ if $\Delta/T_K(0)$ is not too large (Appendix B).^{20,21)} With increasing Δ , the exponent gradually deviates from the universal value to a nonuniversal one, $\text{Min}\{\Gamma_2/\Gamma_1, \Gamma_1/\Gamma_2\}$.¹⁷⁻¹⁹⁾

(iv) On the singlet side ($\Delta < 0$), no Kondo effect is expected when $|\Delta| \gg T_K(0)$. $T_K(\Delta)$ drops to zero suddenly at $|\Delta| \sim T_K(0)$. The behavior of $T_K(\Delta)$ is schematically shown in Fig. 6(b).

5. Conclusions

We have theoretically examined D-D and S-T Kondo effects in multilevel quantum dots. For the D-D Kondo effect, we have considered a quantum dot with two orbitals and spin $1/2$. Using the poor man's scaling method, the Kondo temperature T_K has been evaluated as a function of energy separation Δ between the two orbitals. When the tunnel couplings are equivalent for the

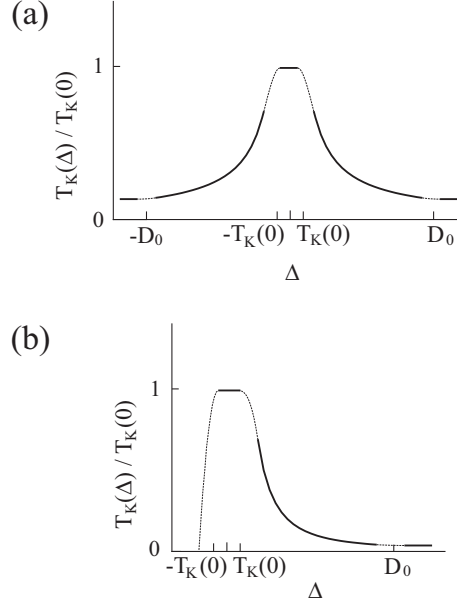


Fig. 6. Schematic drawing of the Kondo temperature T_K , as a function of Δ , for (a) D-D Kondo effect and (b) S-T Kondo effect. $\Delta = \varepsilon_2 - \varepsilon_1$ is the level spacing between two orbitals in (a), whereas $\Delta = E_{S=0} - E_{S=1}$ is the energy difference between spin-singlet and -triplet states in (b). The tunnel couplings are equivalent for two orbitals; $V_1 = V_2$ in eq. (3). T_K is normalized by the Kondo temperature at $\Delta = 0$, $T_K(0)$. D_0 is the bandwidth of conduction electrons in the leads.

two orbitals, $V_1 = V_2$ in eq. (3), $T_K(\Delta)$ is maximal around $\Delta = 0$, and decreases with increasing $|\Delta|$ obeying a power law, eq. (11), with exponent $\gamma = 1$. This behavior of $T_K(\Delta)$ is understood as a crossover from SU(4) to SU(2) Kondo effect. In general case with different tunnel couplings for the two orbitals, $V_1 \neq V_2$, we observe a power law with nonuniversal exponents, reflecting the marginality of the fixed point of SU(4) Kondo effect. We find a relation of $\gamma_L \cdot \gamma_R = 1$, where γ_L and γ_R are the exponents on both sides of a level crossing, as long as $V_1 \sim V_2$.

For the S-T Kondo effect, we have examined a quantum dot with two orbitals and two electrons. The Kondo temperature is maximal around $\Delta = 0$, where Δ is the energy difference between spin-singlet and -triplet states. $T_K(\Delta)$ decreases with increasing $|\Delta|$ in a different way on the triplet side ($\Delta > 0$) or on the singlet side ($\Delta < 0$): $T_K(\Delta)$ approximately shows a power law with $\gamma = 2 + \sqrt{5}$ when $\Delta > 0$, whereas T_K drops to zero suddenly at $|\Delta| \sim T_K$ when $\Delta < 0$.

In both D-D and S-T Kondo effects, the Kondo temperature is maximal around the degeneracy point ($\Delta = 0$), indicating that a total of fourfold spin and orbital degeneracy contributes to the enhancement of the Kondo effect. Now we compare $T_K(\Delta)$ of these Kondo effects in details to explain recent experimental results.²⁴⁾ In the experimental situation of $V_1 \approx V_2$, there are two major differences between them (see Fig. 6).

First, when the energy difference Δ is tuned by a magnetic field, the behavior of $T_K(\Delta)$ is almost symmetric in D-D case and largely asymmetric in S-T case, with respect to the degeneracy point ($\Delta = 0$) in Fig. 1. In the former, T_K decreases gradually with increasing $|\Delta|$ obeying a power law of eq. (11) on both sides of $\Delta > 0$ and $\Delta < 0$. In the latter, $T_K(\Delta)$ approximately obeys a power law on the triplet side ($\Delta > 0$), whereas it drops to zero abruptly on the singlet side ($\Delta < 0$).

Second, the exponent of eq. (11) is about unity in D-D Kondo effect when $V_1 \approx V_2$. The value is smaller than $\gamma = 2 + \sqrt{5}$, the exponent in S-T Kondo effect on the triplet side. Therefore, T_K

decreases with increasing $|\Delta|$ more slowly in D-D case.

In ref. 24, both D-D and S-T Kondo effects have been observed in the same quantum dot with different gate voltage and magnetic field. The enhancement of conductance due to the Kondo effect, ΔG , has been examined in the vicinity of D-D and S-T degeneracy points. As the magnetic field is changed from the degeneracy point, ΔG drops asymmetrically in the S-T case, whereas ΔG decreases more slowly and symmetrically in the D-D case. These behaviors of ΔG are in accordance with our theoretical results of $T_K(\Delta)$ although the direct measurement of $T_K(\Delta)$ has not been reported.

Finally, we comment on the electronic states at $T \ll T_K$. In the D-D Kondo effect, the dot state is represented by a pair of orbital index ($i = 1, 2$) and spin ($S_z = \pm 1/2$). They are fully screened by the electrons in the leads with two conduction channels if $|\Delta| \ll T_K$. In consequence an usual Fermi liquid state of SU(4) symmetry appears in which the orbital and spin degrees of freedom are totally entangled, as discussed by Borda *et al.*⁴²⁾ The Fermi liquid properties are not changed by the marginality of the SU(4) Kondo effect. If $|\Delta| \gg T_K$, the upper orbital is not relevant to the Kondo state. A single channel screens an electron spin in the lower orbital, whereas the other channel is decoupled. Then we should observe a usual Fermi liquid state. Despite the different properties, the conductance through the quantum dot is $G = 2e^2/h$ [apart from an asymmetric factor of two tunnel junctions] in both cases.⁴⁷⁾ (i) When $|\Delta| \ll T_K$, two conduction channels contribute to the transport, but each channel has a phase shift of $\pi/4$ in the SU(4) Kondo effect.^{42,47)} Hence the total conductance is $2e^2/h$. (ii) When $|\Delta| \gg T_K$, a single channel takes part in the transport. The phase shift of $\pi/2$ in the conventional SU(2) Kondo effect (unitary limit) results in $G = 2e^2/h$.

In the S-T Kondo effect, the spin-triplet state is fully screened by two conduction channels. The phase shift of each channel is given by $\pi/2$ in this case. Thus we observe $G = 4e^2/h$ everywhere on the triplet side at $T = 0$. The T dependence of the conductance has been discussed in a special case of $V_1 = V_2$ by Pustilnik *et al.*^{20,21)}

Acknowledgements

The author gratefully acknowledges discussions with Yu. V. Nazarov, L. I. Glazman, H. Hyuga, N. Kawakami, S. Sasaki and S. Tarucha.

Appendix A: Fixed point of D-D Kondo effect

For the D-D Kondo effect, the scaling equations for the exchange couplings, J_1 , J_2 , \tilde{J} , \tilde{T} and T , are given by eq. (12) for $D \gg \Delta$. To find and analyze the fixed point, it is convenient to consider the equations for $j_A = J_A/J_S$, $\tilde{j} = \tilde{J}/J_S$, $\tilde{t} = \tilde{T}/J_S$ and $t = T/J_S$, where $J_S = J_1 + J_2$ and $J_A = J_1 - J_2$. They are given by

$$\frac{dj_A}{dx} = \frac{2j_A}{1 + j_A^2 + 2\tilde{j}(\tilde{j} + \tilde{t})} - j_A, \quad (\text{A.1})$$

$$\frac{d\tilde{j}}{dx} = \frac{\tilde{j} + \tilde{t}/2 + \tilde{j}t}{1 + j_A^2 + 2\tilde{j}(\tilde{j} + \tilde{t})} - \tilde{j}, \quad (\text{A.2})$$

$$\frac{d\tilde{t}}{dx} = \frac{3\tilde{j}/2 + \tilde{t}/2 + \tilde{j}t}{1 + j_A^2 + 2\tilde{j}(\tilde{j} + \tilde{t})} - \tilde{t}, \quad (\text{A.3})$$

$$\frac{dt}{dx} = \frac{3\tilde{j}^2 + \tilde{t}^2}{1 + j_A^2 + 2\tilde{j}(\tilde{j} + \tilde{t})} - t, \quad (\text{A}\cdot 4)$$

with $x = \ln(\nu J_S)$ (we assume that J_S goes to infinity at the fixed point). J_S obeys the scaling equation

$$\frac{d}{d\mathcal{L}}(1/\nu J_S) = 1 + j_A^2 + 2\tilde{j}(\tilde{j} + \tilde{t}), \quad (\text{A}\cdot 5)$$

where $\mathcal{L} = \ln D/D_0$.

From scaling equations, (A.1)–(A.4), we find a fixed point of

$$j_A = 0, \quad \tilde{j} = \tilde{t} = t = 1/2, \quad (\text{A}\cdot 6)$$

with $J_S = \infty$, which corresponds to the fixed point of SU(4) Kondo effect. By the linearization of the scaling equations around the fixed point, we find that the fixed point is marginal. A marginal valuable is j_A .

We derive the power law of $T_K(\Delta)$, eqs. (14) and (15), approximately in the following. First, we expand $1/\nu J_S(D)$ around $D = T_K(0)$ ($\mathcal{L} = \ln T_K(0)/D_0 \equiv \mathcal{L}_K$) at which $1/\nu J_S = 0$. We assume that $\tilde{j} = \tilde{t} = t = 1/2$ (values at the fixed point), whereas the marginal variable j_A is fixed at the initial value, $(V_1^2 - V_2^2)/(V_1^2 + V_2^2)$, at $D = T_K(0)$. To the first order in $\mathcal{L} - \mathcal{L}_K = \ln D/T_K(0)$,

$$\begin{aligned} 1/\nu J_S(D) &\approx \left. \frac{d}{d\mathcal{L}}(1/\nu J_S) \right|_{\mathcal{L}_K} (\mathcal{L} - \mathcal{L}_K) \\ &= (2 + j_A^2)(\mathcal{L} - \mathcal{L}_K). \end{aligned} \quad (\text{A}\cdot 7)$$

For $T_K(0) \ll |\Delta| \ll D_0$, $T_K(\Delta)$ is determined as the energy scale at which $1/\nu J_1 = 0$ in the solution of eq. (13),

$$1/\nu J_1(D) = -2 \ln T_K(\Delta)/D, \quad (\text{A}\cdot 8)$$

Connecting eq. (A.7) [$J_1(D) = J_S(D)(1 + j_A)/2$] and eq. (A.8) at $D = \Delta$, we obtain the power law of eq. (14) with

$$\gamma = \frac{1 - j_A + j_A^2}{1 + j_A} = (V_2/V_1)^2 + O(j_A^2). \quad (\text{A}\cdot 9)$$

This is identical to eq. (15) if j_A^2 is neglected.

Apart from the fixed point (with large Δ), another approximation is taken to explain the power law of $T_K(\Delta)$. We expand $1/\nu J_S$ around the initial point ($D = D_0$, $\mathcal{L} = 0$). By the substitution of the initial values, $j_A = (V_1^2 - V_2^2)/(V_1^2 + V_2^2)$, $\tilde{j} = V_1 V_2/(V_1^2 + V_2^2)$ and $\tilde{t} = 1/2$, into the right-hand side of eq. (A.5), we obtain

$$1/\nu J_S(D) - 1/\nu J_S(D_0) \approx 2\mathcal{L}. \quad (\text{A}\cdot 10)$$

If we connect eqs. (A.10) and (A.8) at $D = \Delta$, we find $T_K(\Delta) \propto \Delta^{-\gamma}$ with exponent of eq. (15). This implies that the power law of eqs. (14) and (15) holds in a wide range of Δ , which is consistent with numerical results shown in Fig. 3.

Appendix B: Fixed point of S-T Kondo effect

For the S-T Kondo effect, the scaling equations (19) for $D \gg \Delta$ are analyzed in the same way as in Appendix A. The scaling equations for $j_A = J_A/J_S$, $\tilde{j} = \tilde{J}/J_S$ and $t = T/J_S$, where

$J_{S/A} = J_1 \pm J_2$, have a fixed point of

$$j_A = 0, \tilde{j} = \sqrt{(2 + \sqrt{5})/2}, t = 1 + \sqrt{5}, \quad (\text{B}\cdot 1)$$

with $J_S = \infty$. This is a stable fixed point.

The scaling equation for J_S is

$$\frac{d}{d\mathcal{L}}(1/\nu J_S) = 1 + j_A^2 + 2\tilde{j}^2, \quad (\text{B}\cdot 2)$$

where $\mathcal{L} = \ln D/D_0$. We expand the solution of eq. (B·2) around the fixed point of eq. (B·1) at which $D = T_K(0)$ ($\mathcal{L} = \mathcal{L}_K$). To the first order in $\mathcal{L} - \mathcal{L}_K = \ln D/T_K(0)$,

$$1/\nu J_S(D) \approx (3 + \sqrt{5})(\mathcal{L} - \mathcal{L}_K). \quad (\text{B}\cdot 3)$$

For $T_K(0) \ll |\Delta| \ll D_0$, we match eq. (B·3) [$J_1(D) = J_2(D) = J_S(D)/2$] and the solution of eqs. (20) at $D = \Delta$,²⁰⁾ and find a power law, eq. (14), with

$$\gamma = 2 + \sqrt{5}. \quad (\text{B}\cdot 4)$$

The universal exponent of the power law is observed in a limited range of Δ in Fig. 5. Far away from the fixed point, we expand $1/\nu J_S$ around the initial point of $D = D_0$ ($\mathcal{L} = 0$). Substituting the initial values, $j_A = (V_1^2 - V_2^2)/(V_1^2 + V_2^2)$ and $\tilde{j} = \sqrt{2}V_1V_2/(V_1^2 + V_2^2)$, into the right-hand side of eq. (B·2), we obtain

$$1/\nu J_S(D) - 1/\nu J_S(D_0) \approx 2\mathcal{L}. \quad (\text{B}\cdot 5)$$

We match eq. (B·5) [$J_{1,2}(D) = J_S(D)(1 \pm j_A)/2$] and the solution of eqs. (20) at $D = \Delta$, we find a power law, $T_K(\Delta) \propto \Delta^{-\gamma}$, with exponent of

$$\gamma = \left(\frac{V_2}{V_1}\right)^2 = \frac{\Gamma_2}{\Gamma_1}, \quad (\text{B}\cdot 6)$$

if $\Gamma_1 \geq \Gamma_2$ ($J_1 \geq J_2$ and hence J_1 diverges faster than J_2), whereas

$$\gamma = \left(\frac{V_1}{V_2}\right)^2 = \frac{\Gamma_1}{\Gamma_2}, \quad (\text{B}\cdot 7)$$

if $\Gamma_1 < \Gamma_2$. Note that $0 < \gamma \leq 1$ in this case. In consequence, the exponent of the power law of $T_K(\Delta)$ changes gradually from the universal value, $2 + \sqrt{5}$, to a nonuniversal one given by eq. (B·6) or (B·7), with increasing Δ , as shown in Fig. 5.¹⁹⁾ This is in contrast to the case of Fig. 3 for the D-D Kondo effect in which a power law with fixed exponent holds in a wide range of Δ .

- 1) J. Kondo: Prog. Theor. Phys. **32** (1964) 37.
- 2) A. C. Hewson: *The Kondo problem to heavy fermions* (Cambridge University Press, Cambridge, 1993).
- 3) K. Yosida: *Theory of Magnetism* (Springer, New York, 1996).
- 4) L. I. Glazman and M. É. Raïkh: Pis'ma Zh. Eksp. Teor. Fiz. **47** (1988) 378 [JETP Lett. **47** (1988) 452].
- 5) T. K. Ng and P. A. Lee: Phys. Rev. Lett. **61** (1988) 1768.
- 6) A. Kawabata: J. Phys. Soc. Jpn. **60** (1991) 3222.
- 7) S. Hershfield, J. H. Davies and J. W. Wilkins: Phys. Rev. Lett. **67** (1991) 3720.
- 8) S. Hershfield, J. H. Davies and J. W. Wilkins: Phys. Rev. B **46** (1992) 7046.
- 9) Y. Meir, N. S. Wingreen and P. A. Lee: Phys. Rev. Lett. **70** (1993) 2601.

- 10) L. P. Kouwenhoven, C. M. Marcus, P. L. McEuen, S. Tarucha, R. M. Westervelt and N. S. Wingreen: in *Mesoscopic Electron Transport*, NATO ASI Series E **345**, eds. L. Y. Sohn, L. P. Kouwenhoven and G. Schön (Kluwer, 1997), p. 105.
- 11) D. Goldhaber-Gordon, H. Shtrikman, D. Mahalu, D. Abusch-Magder, U. Meirav and M. A. Kastner: *Nature* **391** (1998) 156.
- 12) S. M. Cronenwett, T. H. Oosterkamp and L. P. Kouwenhoven: *Science* **281** (1998) 540.
- 13) D. Goldhaber-Gordon, J. Göres, M. A. Kastner, H. Shtrikman, D. Mahalu and U. Meirav: *Phys. Rev. Lett.* **81** (1998) 5225.
- 14) W. G. van der Wiel, S. De Franceschi, T. Fujisawa, J. M. Elzerman, S. Tarucha and L. P. Kouwenhoven: *Science* **289** (2000) 2105.
- 15) S. Sasaki, S. De Franceschi, J. M. Elzerman, W. G. van der Wiel, M. Eto, S. Tarucha and L. P. Kouwenhoven: *Nature* **405** (2000) 764.
- 16) S. Tarucha, D. G. Austing, T. Honda, R. J. van der Hage and L. P. Kouwenhoven: *Phys. Rev. Lett.* **77** (1996) 3613.
- 17) M. Eto and Yu. V. Nazarov: *Phys. Rev. Lett.* **85** (2000) 1306.
- 18) M. Eto and Yu. V. Nazarov: *Phys. Rev. B* **64** (2001) 85322.
- 19) M. Eto and Yu. V. Nazarov: *Phys. Rev. B* **66** (2002) 153319.
- 20) M. Pustilnik and L. I. Glazman: *Phys. Rev. Lett.* **85** (2000) 2993.
- 21) M. Pustilnik and L. I. Glazman: *Phys. Rev. B* **64** (2001) 45328.
- 22) J. Nygård, D. H. Cobden and P. E. Lindelof: *Nature* **408** (2000) 342.
- 23) M. Pustilnik, Y. Avishai, and K. Kikoin: *Phys. Rev. Lett.* **84** (2000) 1756.
- 24) S. Sasaki, S. Amaha, N. Asakawa, M. Eto and S. Tarucha: *Phys. Rev. Lett.* **93** (2004) 17205.
- 25) B. Coqblin and J. R. Schrieffer: *Phys. Rev.* **185** (1969) 847.
- 26) T. Inoshita, A. Shimizu, Y. Kuramoto and H. Sakaki: *Phys. Rev. B* **48** (1993) R14725.
- 27) T. Inoshita, Y. Kuramoto and H. Sakaki: *Superlattices Microstruct.* **22** (1997) 75.
- 28) T. Pohjola, J. König, M. M. Salomaa, J. Schmid, H. Schoeller, and G. Schön: *Europhys. Lett.* **40** (1997) 189.
- 29) W. Izumida, O. Sakai and Y. Shimizu: *J. Phys. Soc. Jpn.* **67** (1998) 2444.
- 30) A. Levy Yeyati, F. Flores and A. Martín-Rodero: *Phys. Rev. Lett.* **83** (1999) 600.
- 31) W. G. van der Wiel, S. De Franceschi, J. M. Elzerman, S. Tarucha, L. P. Kouwenhoven, J. Motohisa, F. Nakajima and T. Fukui: *Phys. Rev. Lett.* **88** (2002) 126803.
- 32) M. Pustilnik and L. I. Glazman: *Phys. Rev. Lett.* **87** (2001) 216601.
- 33) W. Hofstetter and H. Schoeller: *Phys. Rev. Lett.* **88** (2002) 16803.
- 34) M. Pustilnik, L. I. Glazman and W. Hofstetter: *Phys. Rev. B* **68** (2003) 161303(R).
- 35) P. W. Anderson: *J. Phys. C* **3** (1970) 2436.
- 36) P. Nozières and A. Blandin: *J. Phys. (Paris)* **41** (1980) 193.
- 37) D. L. Cox and A. Zawadowski: *Adv. Phys.* **47** (1998) 599.
- 38) F. D. M. Haldane: *J. Phys. C* **11** (1978) 5015.
- 39) K. Yamada, K. Yosida and K. Hanzawa: *Prog. Theor. Phys.* **71** (1984) 450.
- 40) P. Schlottmann: *Phys. Rev. B* **30** (1984) 1454.
- 41) N. Kawakami and A. Okiji: *J. Phys. Soc. Jpn.* **54** (1985) 685.
- 42) L. Borda, G. Zaránd, W. Hofstetter, B. I. Halperin and J. von Delft: *Phys. Rev. Lett.* **90** (2003) 26602.
- 43) T. Kuzmenko, K. Kikoin and Y. Avishai: *Phys. Rev. Lett.* **89** (2002) 156602.
- 44) In our previous papers,¹⁷⁻¹⁹⁾ we have considered a singlet state of $|00\rangle = (C_1 d_{1\uparrow}^\dagger d_{1\downarrow}^\dagger - C_2 d_{2\uparrow}^\dagger d_{2\downarrow}^\dagger)|0\rangle$, where $|C_1|^2 + |C_2|^2 = 1$. In general, $C_2 \neq 0$ owing to the matrix element of the Coulomb interaction between $d_{1\uparrow}^\dagger d_{1\downarrow}^\dagger|0\rangle$ and $d_{2\uparrow}^\dagger d_{2\downarrow}^\dagger|0\rangle$, $\langle 22|e^2/r|11\rangle$. In this paper, we fix $C_1 = 1$ and $C_2 = 0$ to examine the experimental situation of circular dots,²⁴⁾ in which the total angular momentum conserves and hence the matrix element is absent if orbitals 1 and 2 have different angular momentums.
- 45) A lower limit of $T_K(0)$ is given by $D_0 \exp[-1/2\nu(J_1 + J_2)]$.¹⁹⁾
- 46) I. Okada and K. Yosida: *Prog. Theor. Phys.* **49** (1973) 1483.
- 47) R. Sakano and N. Kawakami: private communications.